Magnetoplasmon mode in connected quantum-wire pairs

W. R. Frank, A. O. Govorov,* and J. P. Kotthaus
Sektion Physik, Ludwig-Maximilians-Universität München, Geschwister-Scholl-Platz 1, D-80539 Munich, Germany

C. Steinebach, V. Gudmundsson,† and W. Hansen
Institut für Angewandte Physik, Universität Hamburg, Jungiusstrasse 11, D-20355 Hamburg, Germany

M. Holland
Department of Electronics and Electrical Engineering, University of Glasgow, Glasgow G12 8QQ, United Kingdom
(Received 6 September 1996)

We study the magnetoplasma excitations of field-effect-induced quantum-wire lattices with a unit cell that contains two closely spaced electron channels. The far-infrared-transmission spectra contain an additional mode that is not present in lattices with a simple unit cell investigated previously. We show with a classical model as well as by quantum-mechanical calculations that this mode can be explained by an interwire motion of the electrons that is characteristic for the double-wire system. [S0163-1829(97)51304-X]

Interactions between semiconductor nanostructures such as quantum wires[1–4] and quantum dots[5] are subject to current intensive research. Previous work has focused on Coulomb coupling[1–3] and tunneling.[3,4] In this paper, we report on the manifestation of coupling by direct charge exchange in the magnetoplasmon spectra of parallel quantum wires. The coupling results in an additional resonance at high magnetic fields that dominates the spectrum as the overall electron density increases.

Due to the preparation by holographic lithography,[6] previous research concentrated on quantum wire lattices with evenly spaced channels. The periodicity of the lattice thereby plays an important part in the observable interaction phenomena. Our samples were structured by electron beam lithography, giving us the opportunity to put two closely spaced channels in one unit cell of the lattice, as shown in Fig. 1. The large distance of the wire pairs ensures that we observe only the interaction of two parallel wires, the lattice serving only to enhance the signal-to-noise ratio in the experiment. Figure 1 shows a cross section through a unit cell of the lattice that is periodically repeated in the x direction. The electron system is induced by field-effect beneath the gate electrodes at the interface between the GaAs spacer and an undoped GaAs/AlAs superlattice that serves as barrier versus the gates. The 1.5-μm-thick spacer separates the ionized donors in the Si-doped back contact from the electron system. This increases the mobility of the electron gas.[7,8] The semitransparent gate electrodes consist of an 8-nm-thick NiCr (1:1) layer. From atomic force microscope images we determined the width of the gate stripes to be approximately 150 nm, the smaller distance between the stripes 125 nm, and the larger one 900 nm, yielding an overall period of 1325 nm.

We probe the high-frequency excitations of the wire superlattice with far-infrared (FIR) spectroscopy using a Fourier-transform spectrometer. The FIR transmission experiments require active sample areas that are larger than the writing area of our modified scanning electron microscope. Therefore the active area of 3×3 mm^2 used in our transmission experiments is divided into 49 writing fields each of the size 430×430 μm^2 which are individually exposed with the e-beam writer. In order to ensure that all gates are safely connected, a coarse forklike gate consisting of eight 160-nm-thick Au fingers is prepared with optical lithography prior to the exposure of the writing fields. The writing fields for the e-beam lithography are placed between the fingers of the fork with the stripes running perpendicular to the fingers. At the sides of the writing fields that are connected to the fingers of the fork we added 5-μm-wide stripes in order to avoid imperfect lithography at the junction between the thin wires and the relatively thick fork. Thus in our experiments we always observe, besides the wire modes of interest, a cyclotron resonance that stems from the two-dimensional (2D) electron system under these stripes.

The sample was cooled to 2.2 K and exposed to a constant magnetic field B in the z direction perpendicular to the sample. At magnetic fields above 4 T we clearly resolve a FIR mode with resonance position between the cyclotron resonance frequency and the fundamental intrawire mode of the single wires. In previous FIR experiments with single quantum wire lattices with various periods[6–9] such a mode has not been observed. Figure 2 shows FIR spectra taken at 8

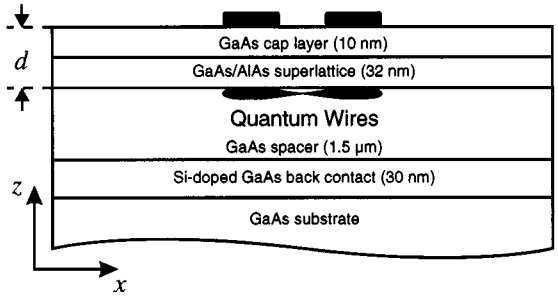

FIG. 1. Schematic cross-sectional view of a unit cell of the wire lattice, showing the epitaxial layers of the heterostructure and the gate layout. Note that the dimensions in the z direction are not to scale.

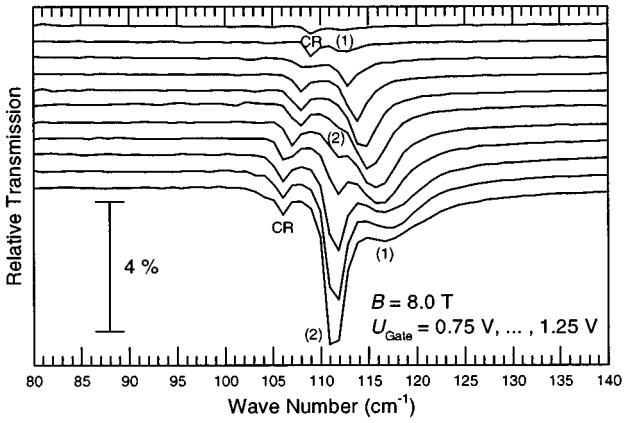

FIG. 2. FIR transmission spectra of a typical sample for gate voltages from 0.75 V to 1.25 V in steps of 0.05 V from top to bottom. The traces are offset for clarity.

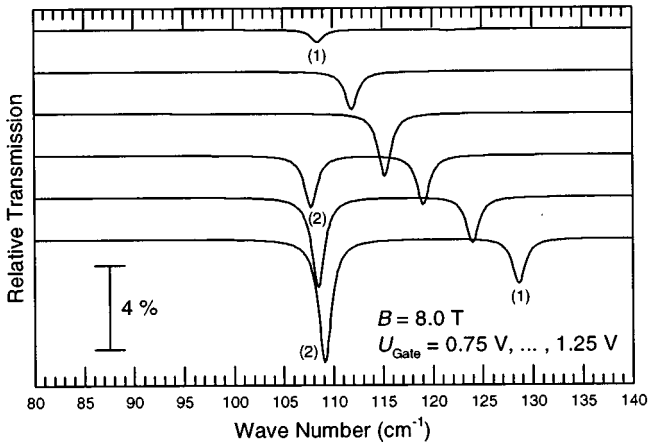

FIG. 3. Relative transmission of the double wire system in the classical model for gate voltages from 0.75 V to 1.25 V in steps of 0.10 V from top to bottom. The traces are offset for clarity.

T and different gate voltages. The peak labeled CR is the cyclotron resonance of the 2D electron system mentioned above. We attribute the shift of the cyclotron resonance from 109 to 106 cm^{-1} to the influence of nonparabolicity effects increasing the electron effective mass from $0.0685m_0$ to $0.0705m_0$.

At 0.75 V, aside from the cyclotron resonance, a weak broad peak labeled (1) at 112.5 cm^{-1} from the wire system is visible. With increasing gate voltage the oscillator strength of this resonance first increases and then decreases slightly for voltages above 1.15 V. The position shifts with increasing gate voltage initially towards higher energy and, within the resolution of the spectra, remains constant for voltages above 1.20 V. At 1.00 V a peak at 112 cm^{-1} (2) appears whose oscillator strength increases rapidly with the gate voltage. In the examined voltage range, no saturation of the oscillator strength of this resonance is visible. Due to experimental constraints, measurements were performed only for gate voltages up to 1.25 V.

In order to elucidate the origin of the different modes we first present a simple classical model. It is valid for the case of high magnetic fields as in the experiments. The electron system is considered to be confined in the (x,y) plane. We assume that with increasing gate voltage the channels are no longer completely separated, but connected by a region of lower electron density. The electron system is described by two parallel stripes of constant two-dimensional electron density n_1 that are connected by another stripe with lower electron density n_2. We describe the total electric field in the x direction including the linearly polarized homogeneous external field and the internal field by

$$E_{\mathrm{tot}}(t,x)=\frac{ed}{\epsilon_r\epsilon_0}\frac{\partial n(t,x)}{\partial x}+E_{\mathrm{ext}}\exp(-i\omega t), \tag{1}$$

where e is the elementary charge, d is the separation between gate and electron system, ϵ_r is the dielectric constant of the semiconductor, ϵ_0 is the vacuum permittivity, and E_{ext} is the amplitude of the external electric field. Here we assumed that the lateral size of the double wire system is large compared to the separation d between the gate and electron system and, for the sake of simplicity, that the surface between the gates is also covered by metal. The 2D electron density n in the system is written in the form $n(t,x)=n_0(x)+\delta n(x)\exp(-i\omega t)$, where $n_0(x)$ is the equilibrium electron density in the channels without excitation (n_1 or n_2 depending on x) and $\delta n(x)\ll n_0(x)$ is the density fluctuation due to the plasmon. In order to calculate the 2D current density in the x direction $j(t,x)=\sigma(\omega,x)E_{\mathrm{tot}}(t,x)$ we use the Drude conductivity obtained from Newton's equations

$$\sigma(\omega,x)=\frac{e^2}{m^*}n_0(x)\frac{i\omega}{\omega^2-\omega_c^2} \tag{2}$$

and get the following differential equation:

$$\frac{\partial^2 j(x)}{\partial x^2}+\frac{m^*\epsilon_r\epsilon_0}{e^2 d}\frac{\omega^2-\omega_c^2}{n_0(x)}j(x)=i\omega\frac{\epsilon_r\epsilon_0}{d}E_{\mathrm{ext}}. \tag{3}$$

Here m^* is the effective mass of the electrons and $\omega_c=eB/m^*$ is the cyclotron frequency. For $E_{\mathrm{ext}}=0$ Eq. (3) is analogous to Schrödinger's equation, giving us a complete set of orthogonal, normalizable eigenfunctions $j_\nu(x)$ from which we construct the solution $j(x)$ of Eq. (3) for the case $E_{\mathrm{ext}}\neq 0$. We then calculate the relative transmission detected in the FIR experiment:

$$\frac{T_{\mathrm{sam}}(\omega)}{T_{\mathrm{ref}}(\omega)}=\left|\frac{1+\sqrt{\epsilon_r}+Z_0\overline{\sigma}_{\mathrm{gate}}}{1+\sqrt{\epsilon_r}+Z_0[\overline{\sigma}_{\mathrm{gate}}+\overline{\sigma}_{\mathrm{eff}}(\omega)]}\right|^2. \tag{4}$$

Here $Z_0=(\epsilon_0 c)^{-1}$ and $\overline{\sigma}_{\mathrm{gate}}$ is an average sheet conductivity that takes into account the gate as well as the back electrodes. The average effective 2D conductivity of the double wire system is

$$\overline{\sigma}_{\mathrm{eff}}(\omega)=\frac{1}{L}\int\frac{j(x)}{E_{\mathrm{ext}}}dx, \tag{5}$$

where L is the period of the gate lattice. Figure 3 shows transmission spectra calculated with Eq. (4). We used the parameters $m^*=0.07m_0$, $\epsilon_r=12.5$, and $\overline{\sigma}_{\mathrm{gate}}=0.005\Omega^{-1}$. From calculations of the bare lateral confining potential we estimate the channels to be approximately 150 nm wide and the distance of the channel centers to be approximately 220

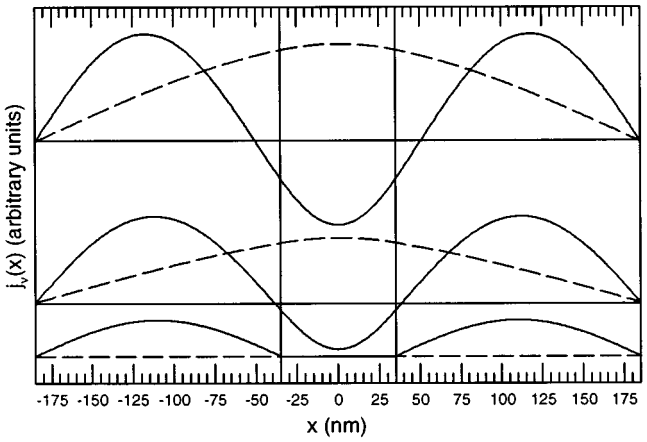

FIG. 4. Current densities of the modes (1) (solid lines) and (2) (dashed lines) calculated in the classical model. Gate voltages: 0.75 V, 1.05 V, and 1.25 V from bottom to top. The traces are offset for clarity. The vertical lines denote the borders between the regions with electron densities n_1 (left and right) and n_2 (middle).

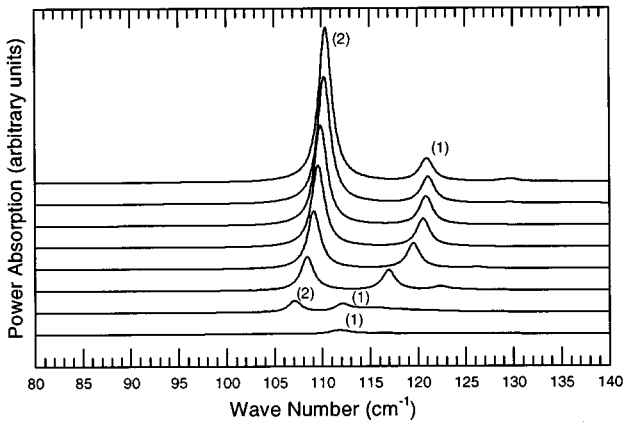

FIG. 5. Absorbed power in the Hartree approximation for 8 different electron densities, $n_{1D}=0.125$, 0.625, 1.125, 1.625, 2.125, 2.5, 3.0, and 3.5×10^7 cm^{-1}. The curves are increasingly offset with increasing density. $B=8$ T, $m^*=0.07m_0$, $T=4$ K, and $\epsilon_r=12.53$.

nm. As an approximation, we assume that the electron densities n_1 and n_2 increase with the gate voltage U_g according to the formula $n_i(U_g)=N(U_g-U_{\rm th}^{(i)})$. From the total oscillator strength of the measured spectra we obtain a value of $n_1\approx10^{11}$ cm^{-2} at $U_g=0.95$ V. The threshold voltages for the channels and the middle region were estimated from the spectra to be $U_{\rm th}^{(1)}=0.70$ V and $U_{\rm th}^{(2)}=0.95$ V, respectively. From these values N is calculated to be $N=4\times10^{11}$ cm^{-2} V^{-1}.

The calculated spectra nicely reproduce the appearance and the increase of the resonance (2) with increasing gate voltage. The values for the oscillator strength are comparable to the measured ones. The marked shift of the mode (1) to higher energies with increasing gate voltage is caused by the rectangular shape of the static electron density distribution. In the experiment, the confinement potential is not rectangular and the width of the double wires increases with the gate voltage. This results in a smaller shift (see below).

Figure 4 shows the calculated current densities $j_\nu(x)$ for the two lowest modes at three different gate voltages. Peak (2) associated with $j_{(2)}(x)$ (dashed lines) is the interwire resonance of the coupled wire system [$j_{(2)}(x)$ has no node], whereas peak (1) associated with $j_{(1)}(x)$ (solid lines) is the intrawire resonance of the individual channels [$j_{(1)}(x)$ has two nodes near the boundaries between the channels and the middle region]. With increasing electron density n_2, mode (1) assumes the character of the first dipole-active harmonic of the wide wire formed by the entire system. Since the oscillator strength of the different modes scales with $[\int j_\nu(x)dx]^2$, the redistribution of the oscillator strength between the modes (1) and (2) is evident from Fig. 4.

For a more quantitative analysis, we have calculated the absorption of the double wire system self-consistently, treating the electron-electron interaction in the time-dependent Hartree approximation.[9,10] We again neglect the spin degree of freedom and consider the electron system to have no extension in the direction perpendicular to the 2D plane. From calculations of the bare confining potential for one wire pair we infer the following formula as an approximation:

$$V_{\rm conf}(x)=\tfrac{1}{2}\hbar\omega_0\left(\frac{x}{l_0}\right)^2\left\{1-\alpha\,\exp\left[-\left(\frac{x}{\beta l_0}\right)^2\right]\right\} \qquad (6)$$

with the parameters $\alpha=2$, $\beta=12$, $\hbar\omega_0=4$ meV, and $l_0=\sqrt{\hbar/(m^*\omega_0)}$. The external electric field is again linearly polarized transverse to the quantum wire. The power absorption is calculated from Joule's law for the self-consistent electric field $E_{\rm sc}=E_{\rm ext}+E_{\rm ind}$, where $E_{\rm ind}$ is induced by the density displacement caused by $E_{\rm sc}$. At zero magnetic field, 17 subbands are occupied for a one-dimensional electron density of 1×10^7 cm^{-1}. For $B=8$ T, one to three Landau levels are occupied, depending on the density. The power absorption in the Hartree approximation is seen in Fig. 5. The spectra are similar to those calculated with the classical model, and are in very good agreement with the experimental data. The oscillator strength distribution between the two resonances is reproduced and the shift of mode (1) shows the same behavior as in the experiment. This contrasts with the classical model and is due to the ''soft'' confinement used in

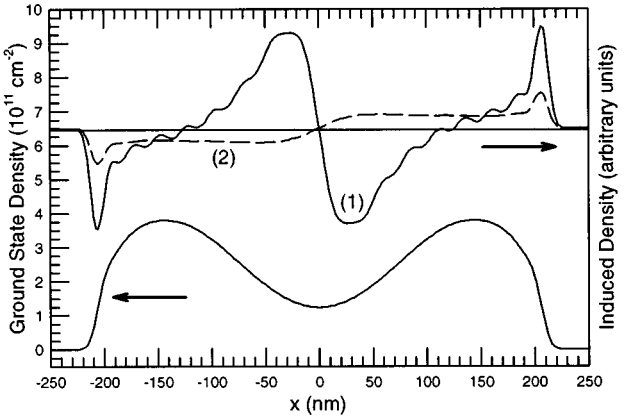

FIG. 6. 2D electron densities in the Hartree approximation for $n_{1D}=1.125\times10^7$ cm^{-1}. Bottom curve and left axis: ground-state density. Top curves and right axis: induced densities for the resonances (1) (solid line) and (2) (dashed line) in Fig. 5. The other parameters are as in Fig. 5.

the calculation that causes a smooth shape of the ground state density that is displayed in Fig. 6, bottom curve.

Peak (2) shows a slight shift to higher energy with increasing density in both the classical and the quantum-mechanical calculations, whereas in Fig. 2, peak (2) apparently does not shift with the gate voltage. This difference is caused by the fact that we neglect the change of the confining potential with increasing gate voltage and do not perform a completely self-consistent device simulation that would be necessary to obtain precise quantitative predictions for the resonance positions. On other samples prepared on a heterostructure with a thicker barrier, we observe a slight shift of feature (2) towards higher energies.

The induced density for peak (1) seen in Fig. 6 (top solid line) has nodes in the middle of each wire, corresponding to the maxima of $j_{(1)}(x)$ in Fig. 4. Hence, the absorption peak (1) corresponds to the lowest dipole-active oscillation mode of the isolated wires. The peak labeled (2) is not present for the isolated wires (Fig. 5, bottom curve), but gains oscillator strength with increasing density when the two electron channels start to overlap. The induced density corresponding to this peak (Fig. 6, top dashed line) has a node between the wires but no node inside a single wire [compare the maximum of $j_{(2)}(x)$ in Fig. 4]. The peak thus occurs at a lower energy than the single-wire mode (1). As the total electron density increases, the induced density of this double-wire mode more and more assumes the character of the fundamental mode of a single wire.

We have also performed classical and quantum-mechanical calculations of the FIR absorption of evenly spaced wires at the transition from isolated wires to a weakly modulated 2D system. For an excitation by a spatially homogeneous electric field in the x direction, a mode corresponding to resonance (2) in our system does not occur because of the periodicity of the lattice. This agrees with the experiments mentioned above.[6,8]

To summarize, we have prepared and studied quantum wire lattices with a complex unit cell. The FIR transmission spectra of the samples show an additional mode not present in quantum wire lattices with a simple unit cell. This mode is explained in terms of a classical model as well as by quantum-mechanical many-body calculations to be caused by charge transfer across the barrier between the wires within a unit cell.

We would like to acknowledge financial support from the following institutions: Deutsche Forschungsgemeinschaft, A. v. Humboldt-Stiftung, Graduiertenkolleg ''Physik nanostrukturierter Festkorper,'' Icelandic Natural Science Foundation, University of Iceland Fund, and the QUANTECS working group of the international collaboration ESPRIT.

*Permanent address: Institute of Semiconductor Physics, Russian Academy of Sciences, Siberian Branch, 630090 Novosibirsk-90, Russia.

†Permanent address: Science Institute, University of Iceland, Dunhaga 3, IS-107 Reykjavik, Iceland.

[1] T. Demel, D. Heitmann, P. Grambow, and K. Ploog, Phys. Rev. B **38**, 12 732 (1988).

[2] T. Egeler *et al.*, Phys. Rev. Lett. **65**, 1804 (1990).

[3] W. Que, Phys. Rev. B **43**, 7127 (1991).

[4] T. V. Shahbazyan and S. E. Ulloa, Phys. Rev. B (to be published).

[5] C. Dahl, J. P. Kotthaus, H. Nickel, and W. Schlapp, Phys. Rev. B **46**, 15 590 (1992).

[6] W. Hansen *et al.*, Phys. Rev. Lett. **58**, 2586 (1987).

[7] H. Drexler *et al.*, Phys. Rev. B **46**, 12 849 (1992).

[8] G. Hertel *et al.*, Solid-State Electron. **37**, 1289 (1994).

[9] V. Gudmundsson *et al.*, Phys. Rev. B **51**, 17 744 (1995).

[10] A. Brataas, V. Gudmundsson, A. G. Mal'shukov, and K. A. Chao, J. Phys., Condens. Matter. **8**, 4797 (1996).